Improving Lander Leg Stability for Precision Landing on the Moon

Ronald H. Freeman, PhD
Space Operations and Support Technical Committee, AIAA

Abstract
Although the lighting conditions do not affect the performance of the touchdown system, they are critical for the power subsystem. Therefore, the flight system's Hazard Detection and Avoidance (HDA) sub-system needs to avoid unfavorable hazards of slope and roughness, and the potentiality thereof posed by the local shadowing in the landing zone. Since the descent and ACS propulsion systems use pulsed thrusters, the vertical touchdown velocity and the tilt angle and rates may not be completely nulled at touchdown. Legged landers are designed to touch down in a defined attitude on their landing legs. The analysis of the terrain-related failure probabilities remains incomplete without knowledge about the geotechnical properties of the landing site such as the terrain slope and roughness. This paper aims to investigate the approaches used to sense the terrain during descent and augment the inertial navigation by providing, in real-time, position or bearing estimates relative to known surface landmarks.
Keywords: Terrain relative navigation, landing safety assessment, digital terrain model

I. Introduction
The landing of a spacecraft on the surface of a planetary body is one of the greatest challenges in space exploration endeavors. This results from the task of decelerating the vehicle in a relatively short period of time from its orbital entry velocity to a complete rest on the Moon's surface. Narrow targets for the spacecraft position, velocity and attitude must be met for a controlled landing within the functional capabilities. As typically no ground control intervention is possible, a high degree of automation and autonomy is needed. The narrow band for the states and time of spacecraft criticality makes the mission phase hardly fault tolerant. The design of the system and its later operation are strongly affected by a planetary environment whose descriptors are still to some degree uncertain. The environment, giving the context in which the spacecraft operates, is entirety from gravity field, atmosphere, illumination conditions and surface properties. Although the lighting conditions do not affect the performance of the touchdown system, they are critical for the power subsystem. Therefore, the flight system's Hazard Detection and Avoidance (HDA) sub-system needs to avoid unfavorable hazards of slope and roughness, and the potentiality thereof posed by the local shadowing in the landing zone. In order to emulate a certain lighting condition for the HDA-driven landing dispersion, a NAC ortho-image (DLR-CR1-NACORT03 based on LRO image M139817894L) is taken. The landing zone represents an illumination condition with a sun azimuth of 143.3° and an elevation of 1.12° at the CR nominal coordinates [1].

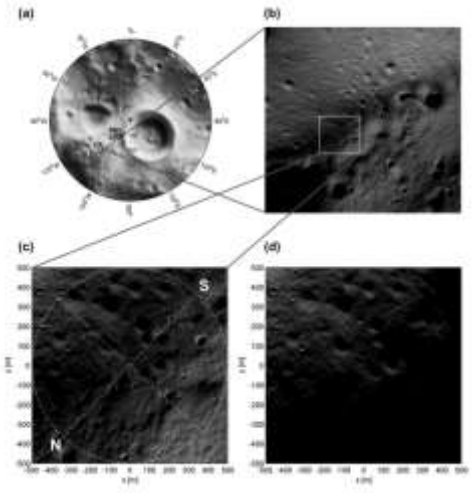

Figure 8-2 Landing site Connecting Ridge«: (a) located in the Lunar South Pole vicinity, (b) Connecting Ridge region (5×5km² image mosaic), (c) landing zone 1×1km², and (d) landing zone with an example for illumination conditions.

Adler, M., et al. (2012) defined "Entry, Descent and Landing (EDL) as encompassing "the components, systems, qualification and operation to safely and usefully bring a vehicle from approach conditions to contact with the surface of a solar system body" [2]. On one side, the landing system is characterized by engineering constraints marking the spacecraft's capability to attain and accommodate a specific landing site. A mission design neglecting these constraints is prone to a landing failure. Consequently, scientific opportunities will be lost. On the other hand, the science case requires spacecraft to land in an area suitable to meet the science objectives. Legged landers are designed to touch down in a defined attitude on their landing legs. Energy dissipation and load attenuation is realized by absorber elements inside or attached to the stroking struts. The touch down velocities are well below 10 m/s for which reason these landing systems are also sometimes dubbed "soft" landers. The importance of this concept is the key rationale for an exceedance of the functional limits as regarded "failure" which is defined in ECSS 2004 as "the termination of the ability of an item to perform a required function". Furthermore, failures are classified by Birolini (1997) according to their mode (the local effect or symptom), their cause and their effect (the consequences) [3]. The failures of the landing platform are coarsely described in Table 2-2.

Mode	Cause	Effect
The landing platform tips over.	The landing is dynamically unstable.	Loss of mission.
Excessive loads and/or shocks to the system and/or payload.	The energy absorption capability has been exceeded.	Potential of damage to system and/or payload resulting in partial or complete degradation of mission.
Ground contact with parts other than the footpads	The ground clearance has been insufficient to accommodate the terrain.	Potential of structural damage and/or impairment of the surface operations.

Table 2-2 Legged landing platform touchdown failure modes, causes and effects

In a touchdown event the shape and surface conditions of the landing site determine significantly the touchdown dynamics of the landing system. The development of landing site assessment in more than 40 years of planetary exploration has shown that high resolution image data is indispensable for the necessary characterization.

Problem

Intuitive Machines -1 assessment of Odysseus not so soft-landing on the Moon determined the inoperability of the laser rangefinders on the spacecraft, and that software was modified to use lasers on a NASA payload, the Navigation Doppler Lidar, instead. However, Tim Crain, Intuitive Machines' chief technology officer, said that while engineers successfully mapped the data from the NASA payload into their software, they missed a data flag in the software to validate the data. "Basically, we landed with our IMU [inertial measurement unit] and our optical navigation data flow algorithms," he said. Without altimetry data from a laser rangefinder, the lander ended up descending just short of its landing site, in an area about 1.5 kilometers away with higher terrain. "We came in with more downward velocity and more horizontal velocity," CEO Altemus said. The lander thought it was higher above the surface than it actually was. "We hit harder and sort of skidded along the way," he said. "We sat there upright with the engine firing for a period of time, and then as it wound down, the vehicle just gently tipped over." The landing took place on a 12-degree slope, causing the lander to rest at an angle of about 30 degrees off the surface as a helium tank or other component hit the surface [4].

Purpose

Precise landing on the surface of the Moon enables intended space missions to get closer to a point of interest. However, traditional lunar landing approaches, based on inertial sensing, do not have the navigational precision to meet this goal. To address this shortcoming, several terrain relative navigation (TRN) approaches have been proposed. This paper aims to investigate the approaches used to sense the terrain during descent and augment the inertial navigation by providing, in real-time, position or bearing estimates relative to known surface landmarks.

From these estimates, the navigational precision can be increased to a level that meets the requirement of landing within 90 m of a predetermined location [5] and lander leg stability maintained.

II. Methods and Results

A literature survey was conducted relevant to TRN approaches. Digital Terrain Model (DTM) basically stored terrain elevation data in a gridded data format. The introduction of the algorithmic DTM evaluation was restricted only to terrain properties with relevance for the mechanical interaction with what appeared as the slope and roughness of the terrain. The algorithms were coded using the scientific computing language MATLAB. Two different cases: (i) a simple 2-dimensional (2D) example and (ii) a more realistic 3D parameterized models for crater and boulder. In the 2D verification case, five arbitrarily chosen data points with spacing of 2m provided a reference or ground truth terrain model. Its true elevation was determined by a linear equation with some superimposed variance and an additional roughness value (a "boulder") at the position x = 2m. The associated parameters are given in Table 7-1 in the column "Ground Truth Reference Data".

	Ground Truth Reference Data	Estimate w/o Outlier Detection	Estimate with Outlier Detection
Slope [°]	5.0	7.0	5.3
Roughness [m]	0.56	0.42	0.60
1σ-Error [m]	0.10	0.26	0.12

Table 7-1 Algorithm verification – 2D example – estimated versus true properties

The reflective properties of the terrain depend on its material composition, microscopic surface roughness and the angular relations between the sun, the terrain surface and the receiver. Changes in reflectivity differentiate surface features. State-of-the-art imaging systems belong to the group of line scanners, which scan the surface underneath the orbit's trajectory with a sensor (e.g. charge-coupled device) where the pixels are arranged in a line. The path from the measured raw data to a digital terrain model requires several processing steps. First, the raw data received from the space segment are brought into a decompressed format (a level 1 product). Then, several corrections are applied to the data including radiometric and geometric calibrations. This level 2 considers the spacecraft position and orientation allowing an assignment of image pixel to geodetic coordinates of the planetary body. The projection of a three-dimensional object onto a two-dimensional receiver plane inevitably leads to distortions including parallaxes effects of different terrain sections. Its correction requires priori information on the true shape of that terrain section. Such terrain elevation data is typically provided by laser altimetry: active ranging systems emit a signal and measure the time of flight of the reflected signal, which allows determining the distance to the surface. Knowledge of spacecraft's position enables reconstructing the three-dimensional terrain profile. Correcting the terrain shape-induced image distortions using such digital terrain model (DTM), leads to an ortho-rectified or level 3 data product. Laser altimetry-derived DTM typically resolves several meters which is not sufficient to identify potential hazardous terrain features on a lander scale level. This situation can be improved using stereo-imaging techniques. Stereo image pairs can be either obtained from different orbits with overlapping camera swath or directly by dedicated stereo-cameras such as the HRSC camera described by Scholten et al. (2005) [6]. The subtle differences in the parallaxes of the same terrain section when imaged from different positions, however, provide a starting point to reconstruct the depth information. The production process towards a DTM generated from stereo image pairs starts with a pre-rectification of the individual images. This step utilizes laser altimeter data that was DTM-based. The same points on the surface, observed from different and known orbit positions, provides reconstruction of the depth information in the image. Transformation of the three-dimensional coordinates into planetary body fixed latitude, longitude, and height values, suitable for map projection, completes the processing chain. Data products involving such deeper processing are so called level 4 products [7]. Image resolutions in the

sub-meter range enable the required DTM resolution in the lander scale range. Such DTM and ortho-image generation, specifically with regard to the lunar case, was described by Oberst et al. (2010) [8]. The underlying lunar image data products were generated by the Lunar Reconnaissance Orbiter Camera (LROC) delivering images with a resolution of around 0.5m [9].

Terrain Slope and Roughness

Determination of terrain properties potentially hazardous to the landing platform describes the terrain slope and its roughness. They significantly influence the mechanical contact at touchdown between the planetary surface and the landing system. Slope is defined by Johnson et al. 2002 as "the angle between the robust plane normal vector and the gravity vector" [10] or by De Rosa et al. 2012 as "the inclination relative to the local horizontal of the mean plane" [11]. The robust or mean plane is thereby the least error fit to the terrain surface underneath the landing system footprint. Roughness is defined as "the deviation from the mean plane and as such is a property of each point of the terrain below the lander …" [12] or the "difference between the robust plane and the elevation map" [13].

3D verification case

While the terrain property "slope" is unambiguously defined as the inclination of the mean plane with respect to the gravity vector, the case for the terrain property "roughness" is less clear. Roughness, defined as deviation from the mean plane, can be caused by many different geological processes. Besides this measurable deviation, roughness is also characterized by a certain shape associated with its geological nature. Therefore, generic models for craters and boulders are introduced to investigate their impact on the terrain property estimation as they are the most prominent sources of roughness. Pike 1977 has shown that the size and shape of simple, bowl-shaped crater depend only from the kinetic energy of the impacting body, but – unlike complex crater – not from the gravity of its planetary target body [14]. The forming of the crater bowl and rim follows a self-similar pattern. The rim height and the depth of the bowl can be mathematically described as a fraction of the crater diameter.

Lander leg stability

Fig. 3 flowchart shows the process of designing the landing legs and thrust force and conducting the landing operation. As shown in Fig. 3, the design method comprises three steps. First, design the desired foot stiffness and damping coefficients. Then, decompose the coefficient values into horizontal and vertical components. Finally, convert the metrics from Cartesian space to joint space, and acquire the stiffness and damping coefficients of leg joints.

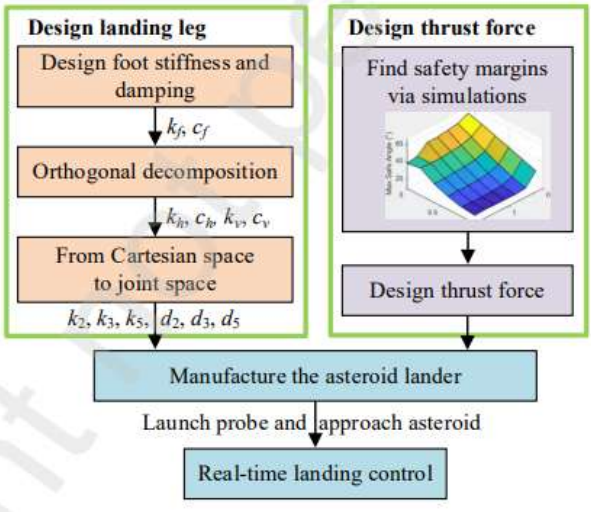

Figure 3.

In practice, the landing leg's nonlinearity, the lander's attitude error, and rough terrain cause the lander to rebound. The thruster at the body's top will generate a downward propelling force that suppresses the rebound motions. As shown in Fig. 3, the design stage includes finding the safety margins and designing thrust force [15]. In the landing operation, the thruster is controlled in real-time. Since the contact forces between the footpads and the ground surface are discontinuous and unpredictable, it is challenging to analyze the lander's stability using the stability

criteria in control theories. From the simulation results, a lightweight thruster provides a proper thrust force value that ensures the lander's stability. In the landing operation, the inertia sensor of the lander measures the body's vertical acceleration. Meanwhile, force sensors of the landing footpads measured the ground contact forces. The lander's onboard computer starts the thruster when it detects a merge of acceleration or contact force, indicating the lander collided with the ground. A simple control strategy would be for the thruster to output a constant propelling force of F_{thr} and not stop until the lander achieves stability or has anchored on the surface.

Although some landers have successfully landed on the moon [16], landing is still an immature field and requires further research to improve its success rate. Buffer legs may accomplish a soft landing. The main body of the lander is equipped with three or four buffer leg mechanisms, which are composed of some struts and a footpad. When the footpads touch down the ground, buffer materials that fill in the struts will absorb part of the shock energies to protect the main body from damage. During the landing process, intricate connections between the struts, nonlinear buffer materials, and the interactions between the footpad with complex shape and irregular ground, result in complex dynamics responses, which are worth studying thoroughly to ensure the safety and stability of a landing. A dynamical model for the soft landing of a space lander consists of a main body and four sets of buffer mechanisms. Each buffer mechanism includes one primary strut and two secondary struts. The primary strut is linked with the main body through a cantilever beam and fixed with the footpad. The secondary strut is made up by an outer tube jointed with the main body and an inner tube jointed with the footpad. Between the outer and inner tubes, buffer materials are filled to absorb the shock energy. Degrees of freedom of the main body and four footpads are generalized as coordinates. Generalized coordinates describe motions of the struts in the buffer mechanisms, such as the offset displacement of the primary strut and the compression lengths of the secondary struts. Therefore, the interaction force between the primary strut and the main body and the compression force between the inner and outer tubes in the secondary struts may be calculated. The contact force between the footpad and the ground can be obtained by applying the Archimedes law for granular media to the discrete elements of the footpad.

The Warm Gas Test Article (WGTA), a test lander developed to demonstrate the terminal descent phase of the landing was used to test lander control algorithms for the critical last minutes of the mission prior to landing. The WGTA lander, shown in Fig.1, is derived from a robotic lunar lander (RLL) baseline design and consists of a flight-like structure at its core and incorporates flight-like Guidance, Navigation and Control (GNC) sensors. Details regarding the WGTA and flight tests can be found in [17]. The design and development of the leg assembly was structured to satisfy the WGTA requirements. During the RLL effort, design requirements were generated for several mission concepts with a range of instruments, and these were used to perform a series of trades. The progression of trades led to a common baseline system architecture for most of the mission concepts studied, and this evolved into more detailed subsystem level requirements, as described in [18]. The requirements for the RLL leg were mostly driven by the kinematic state of the lander at touchdown and were jointly developed by the mechanical and GNC teams. This was further modified to support the earth-based flight tests of the WGTA.

Figure 1. Warm Gas Test Article

The leg-based landing system follows preliminary configuration trades as described in [19]. After finalizing the top-level requirements and conceptual design, another set of trades requires the development of the details. Some of these trade studies are discussed here.

- Number of Legs. One of the first trades determines the number of leg assemblies. In the past, most unmanned smaller landers had three legs, while the Apollo mission's Eagle had four legs. The key driver for the number of legs is stability. Stability analysis uses analytical techniques discussed in [20].Factors influencing stability include the lander configuration (mass, CG height, number of legs and lander foot pad radius) and the landing kinematics (horizontal and vertical landing velocities, lander rotational rates, lander attitude and landing surface inclination). A three-leg configuration provides sufficient stability and margins. Adding a fourth leg improves stability but not enough to justify increased mass and complexity.

- Energy Absorption Mechanisms. Energy dissipation and load attenuation is realized by absorber elements inside or attached to the stroking struts. The most common design is to use a crushable medium packed telescoping tubes. Upon impact, this medium gets compressed by applying a constant force that decelerates the lander. These materials are effective in absorbing energy in compression only, yet additional required mechanisms will use these materials to absorb energy in tension. Another approach incorporates a hydraulic damper. They are self-resetting and do not need refurbishment after each landing. Comparative evaluation of both techniques selects a combination of a hydraulic damper and a crushable medium as the energy absorbing elements in the primary strut.

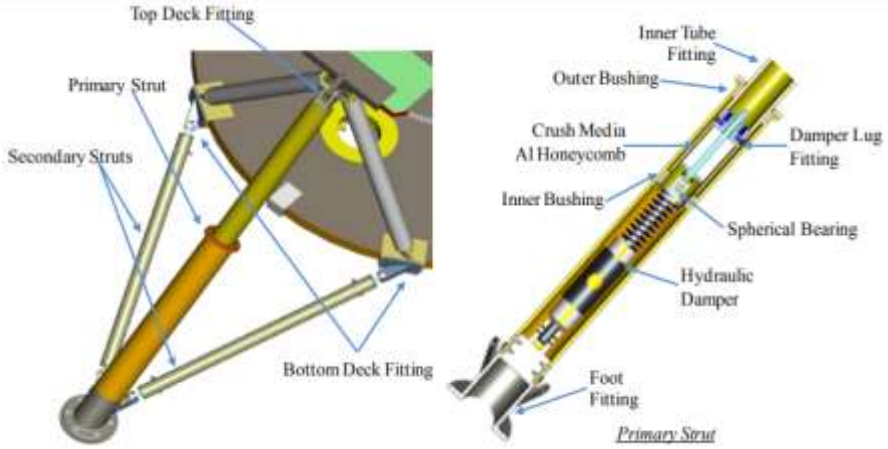

Figure 2. Leg Assembly Details

The landing safety assessment is an integral element of the planning of a planetary landing mission. In addition to the position dispersion around the nominal landing site, it has to consider the topographic characteristics of the area which might endanger the landing system. A mathematical method, adopted from reliability engineering methods, has been developed in order to determine these terrain-related failure probabilities from touchdown dynamics data. A legged landing platform is used as a study object. Its touchdown dynamics is represented by a high-fidelity numerical multibody simulation which is validated by experimental data from a dedicated test campaign. The numerical simulation then provides the input data for the analysis process. However, the analysis of the terrain-related failure probabilities remains incomplete without knowledge about the geotechnical properties of the landing site such as the terrain slope and roughness. This information is obtained from a landing site characterization extracted from high resolution digital terrain models considered of a specific base length determined by the landing platform's footprint. [21].

Since the descent and ACS propulsion systems use pulsed thrusters, the vertical touchdown velocity and the tilt angle and rates may not be completely nulled at touchdown. In addition, the lunar surface is highly variable with terrain features such as slopes, rocks, and craters which the landing legs must accommodate. Non-linear kinematic math models have been produced for the flight lander to predict the behavior of the lander at landing and optimize the design. A test program is underway to validate these models. The testing is in three phases: 1) A simple rigid block lander, 2) A 1/2 scale lander model of a flight lander with elastic deformation and 3) The same ½ scale model with inelastic energy absorption systems. Math models were developed for each of these configurations and test data will be used to compare to the analytic results. To date the first phase (rigid block) of testing has been completed. The test results agreed very well with the analytic predictions. The ½ scale model and the associated test equipment are in final assembly and testing will begin soon [22].

III. Discussion

The TRN approach presented here, based on correlation of LIDAR data and an elevation map, meets the objective of 90 m landing precision under any lighting conditions. Experiments with field test data provide TRN estimates having errors typically less than 50 m. Most incorrect estimates were eliminated using confidence metrics based on terrain relief and correlation statistics. Instrument misalignments were the main causes of large global errors. Disregarding those, more than 95% of the TRN estimates passed on to the navigation filter were accurate.

Furthermore, the algorithm was able to handle initial position uncertainty of 1.6 km without performance degradation. However, TRN performance degraded with larger map pixel sizes. Future work will include a study of the effect of contour width on TRN performance. Also, pre-filtering of the contours though a band-pass filter or masking out flat regions will be investigated to sharpen the correlation peak [23].

A new center of gravity (COG) trajectory planning algorithm combined Jacobian COG with a centroid of a support polygon, to include a foot contact constraint [24]. This strategy effectively balances optimization and search operations, improving the lander's passing ability and stability in complex terrains. Moreover, this work considers the longitudinal stability margin (LSM) method and minimum stability margin of the lander as a sequential optimization problem. Hence, the hierarchical control architecture is established to compensate for the mission and environment changes, improving computational efficiency [25]. Finally, the developed method applies to the simulation prototype to verify its performance in various environments. The experimental results demonstrate that the proposed method allows the lander to move in various environments.

IV. Conclusion

Although the lighting conditions do not affect the performance of the touchdown system, they are critical for the power subsystem. Therefore, the flight system's Hazard Detection and Avoidance (HDA) sub-system needs to avoid unfavorable hazards of slope and roughness, and the potentiality thereof posed by the local shadowing in the landing zone. Since the descent and ACS (attitude control system) propulsion systems use pulsed thrusters, the vertical touchdown velocity and the tilt angle and rates may not be completely nulled at touchdown. Legged landers are designed to touch down in a defined attitude on their landing legs. The analysis of the terrain-related failure probabilities remains incomplete without knowledge about the geotechnical properties of the landing site such as the terrain slope and roughness. This paper aims to investigate the approaches used to sense the terrain during descent and augment the inertial navigation by providing, in real-time, position or bearing estimates relative to known surface landmarks.

References

[1] Scholten, F., et al. (2012). *Connecting Ridge Potential Landing Site for ESA Lunar Lander*. NAC_DTM_ESALL _CR1.
[2] Adler, M., et al. (2012). *Entry, Descent and Landing Roadmap*, *Technology Area 09*. NASA.
[3] Birolini, A. (1997). Quality and Reliability of Technical Systems. *Theory, Practice, Management*. 2nd Edition, Springer.
[4] Foust, J. (February 28, 2024). *Intuitive Machines and NASA call IM-1 lunar lander a success as mission winds down.* Retrieved from www.spacenews.com.
[5] Epp, C. & Smith, T. (2008). The Autonomous Precision Landing and Hazard Detection and Avoidance Technology (ALHAT). *Aerospace Conference*, Big Sky, MT, March 2008, pp. 1-7.
[6] Scholten, F., et al. (2005). Mars Express HRSC Data Processing – Methods and Operational Aspects. *Photogrammetric Engineering & Remote Sensing 71*(10), 1143–1152.
[7] Scholten, F., et al. (2005). Express HRSC Data Processing – Methods and Operational Aspects. *Photogrammetric Engineering & Remote Sensing 71*(10), 1143–1152.
[8] Oberst, J., et al. (2010). Apollo 17 Landing Site Topography from LROC NAC Stereo Data –First Analysis and Results. *41st Lunar and Planetary Science Conference, No. 2051*.
[9] Robinson, M., et al. (2010). Lunar Reconnaissance Orbiter Camera (LROC). *Instrument Overview. Space Science Reviews 150*(1-4), 81–124.
[10] Johnson, A., et.al. (2002). Lidar-Based Hazard Avoidance for Safe Landing on Mars, *Journal of Guidance, Control, and Dynamics 25*(6).
[11] de Rosa, D., et al. (2012). Characterization of potential landing sites for the European Space Agency's Lunar Lander project. *Planetary and Space Science 74*.
[12] de Rosa, D., et al. (2012). Characterization of potential landing sites for the European Space Agency's Lunar Lander project. *Planetary and Space Science 74*.
[13] Johnson, A., et.al. (2002). Lidar-Based Hazard Avoidance for Safe Landing on Mars, *Journal of Guidance, Control, and Dynamics 25*(6).
[14] Pike, R. (1977). Size-dependance in the shape of fresh impact craters on the moon. in: D.J. Roddy et.al (eds.), *Impact and Explosion Cratering*, Pergamon Press, pp.489-509, New York / USA.

[15] Shi, T., Yang, Y., Zhang, Z., Liu, C., Liu, C., & Ma, D. (2024). Soft-landing dynamics of a type of four-legged space lander. *Aerospace Science and Technology*, *150*, 109217.
[16] Zhang, B., Tang, S., & Pan, B. (2016) Multi-constrained suboptimal powered descent guidance for lunar pinpoint soft landing. *Aerospace Science and Technology 48*, 203–213.
[17] Chavers G., et al. (2010). *Robotic lunar landers for science and exploration*, IPPW-7.
[18] Cooper S., et al. (2010). *Development of a lightweight, energy absorbing soft-landing system for robotic probes*, IPPW-7.
[19] Cooper S., et al. (2010). *Development of a Lightweight, Energy Absorbing Soft-Landing System for Robotic Probes,* IPPW-7.
[20] Walton Jr. E.C., et al. (1964). Studies of touchdown stability for lunar landing vehicles, *J. Spacecraft, 1*, 552-556.
[21] Witte, L. (2015). *Touchdown dynamics and the probability of terrain related failure of planetary landing systems-a contribution to the landing safety assessment process* (Doctoral dissertation, University of Bremen).
[22] Chavers, D., Cohen, B., Bassler, J., Hammond, M., Harris, D., Hill, L, ... & Reed, C. (2010). Robotic Lunar Landers for Science and Exploration. In *7th International Planetary Probe Workshop* (IPPW-7) (No. M10-0698).
[23] Johnson, A., & Ivanov, T. (2011, August). Analysis and testing of a lidar-based approach to terrain relative navigation for precise lunar landing. In *AIAA guidance, navigation, and control conference* (p. 6578).
[24] Neuhaus P., Pratt J., Johnson, M. (2011). Comprehensive summary of the institute for human and machine cognition's experience with Little-Dog. *The International Journal of Robotics Research 30*(2), 216-235.
[25] Zhou, J., Ma, H., Chen, J., Jia, S., & Tian, S. (2023). Motion characteristics and gait planning methods analysis for the walkable lunar lander to optimize the performances of terrain adaptability. *Aerospace Science and Technology*, *132*, 108030.